Papers in Natural Resources   Natural Resources, School of

2008

A Coupled MM5-Noah and Surface Model-Based Assessment of Sensitivity of Planetary Boundary Layer Variables to Anomalous Soil Moisture Conditions

Rezaul Mahmood
University of Nebraska - Lincoln

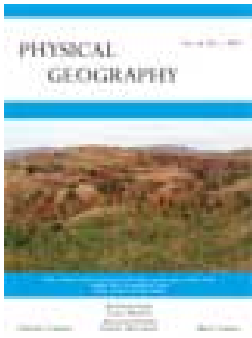# A Coupled MM5-NOAH Land Surface Model-based Assessment of Sensitivity of Planetary Boundary Layer Variables to Anomalous Soil Moisture Conditions

Arturo I. Quintanar , Rezaul Mahmood , John Loughrin & Nanh C. Lovanh

A COUPLED MM5-NOAH LAND SURFACE MODEL–BASED ASSESSMENT OF SENSITIVITY OF PLANETARY BOUNDARY LAYER VARIABLES TO ANOMALOUS SOIL MOISTURE CONDITIONS

*Arturo I. Quintanar** and *Rezaul Mahmood*
Department of Geology and Geography and Kentucky Climate Center
Western Kentucky University
Bowling Green, Kentucky 42101

John Loughrin and *Nanh C. Lovanh*
USDA-ARS, Animal Waste Management Research Unit
Bowling Green, Kentucky 42101

Abstract: The sensitivity of the near-surface weather variables and small-scale convection to soil moisture for Western Kentucky was investigated with the aide of the MM5 Penn State/NCAR mesoscale atmospheric model for three different synoptic conditions in June 2006. The model was initialized with FNL reanalysis from NCEP containing soil moisture data calculated with the Noah land surface model. Dry and wet experiments were performed in order to find the influence of soil moisture specification on boundary layer atmospheric variables. Dry experiments showed less available atmospheric moisture (between 2 and 6 g kg^{-1}) at near-surface levels during all synoptic events consistent with slightly deeper boundary layers, higher lifting condensation levels and a larger Bowen ratio. As expected, precipitation rates were generally smaller than those of the control simulation. However, during a moderately strong synoptic event in early June, the dry experiments displayed larger precipitation rates compared to the control experiment (up to 5 mm in 3 hr) as the soil volumetric fraction was decreased from 0.05 to 0.15 (m^3 m^{-3}) with respect to the control simulation. Precipitation rates in wet experiments were also modulated by characteristics of synoptic conditions. In early June, precipitation rates slightly were larger than the control run (from 0.2 mm 3 h^{-1} to 1.4 mm 3 h^{-1}) while in the other periods precipitation was reduced significantly. Both dry and wet anomaly experiments experienced reduced precipitation for different reasons. It was found, lifting condensation level, CAPE and low Bowen ratio were not sensitive markers of changes in soil moisture. Equivalent potential temperature was a better indicator of precipitation changes among all experiments. The controlling factor in these responses was the soil moisture content forcing vertical velocities. Thermodynamic conditions such as local stability played a less substantial role in controlling the precipitation processes. It was found that the response of planetary boundary layer variables under a variety of soil moisture conditions can be modified due to degree of synoptic forcing. Weak-to-moderate forcing favored convection while strong synoptic forcing tended to suppress it under dry soil moisture conditions. Wetter soils did not produce a response in horizontal wind fields as large as under the drier soils. [Key words: soil moisture, regional modeling, land surface-atmosphere interactions.]

INTRODUCTION

It has long been recognized that the coupling between the atmosphere and land processes can impact atmospheric forecasts at almost all time and spatial scales of

---

*Corresponding author.

54

practical interest. Early climate studies have dealt with the presence of ocean and land processes in order to be able to account for the observed climate over land and to close the water budgets globally (Mintz, 1984; Delworth and Manabe, 1988). At shorter time scales, and at the regional scales, many modeling as well as a few observational studies have shown that the atmosphere is sensitive to soil moisture, land use, and vegetation cover (Anthes, 1984; Clark and Arrit, 1995; Beljaars et al., 1996; Findell and Eltahir, 1997; Pal and Eltahir, 2001; Pielke, 2001; Alonge et al., 2007).

Soil moisture changes affect the availability of water for evapotranspiration from vegetation and bare soil. Consequently, sensible and latent heat fluxes or, equivalently, the Bowen ratio (the ratio of sensible to latent heat flux) are affected. A small Bowen ratio together with horizontal gradients of soil moisture and a lifting mechanism can generate deep cumulus convection under certain conditions (Anthes, 1984; Lanicci et al., 1987; Segal and Arrit, 1992; Segal et al., 1995; Betts et al., 1996; Pielke, 2001). The effect of soil moisture changes on precipitation and deep convection at the regional scale has also been the focus of several studies (e.g., Betts et al., 1996; Pal and Eltahir, 2001; Findell and Eltahir, 2003; Sutton et al., 2005; Aligo et al., 2007; Alonge et al., 2007). In general, it is found that wetter soils enhance the possibility of cloud cover and potential for convection by increasing the amount of moist static stability on shallower atmospheric boundary layers. Over drier soils, increased sensible heat fluxes force a deeper boundary and in some cases (e.g., weak stability above the boundary layer), can increase the potential for cloud formation (Ek and Mahrt, 1994; Ek and Holstag, 2004).

The influence of soil moisture on wind has only been studied in connection with surface heterogeneity (Ookuchi et al., 1984; Segal and Arrit, 1992). An attempt to connect the state of the near-surface wind field to soil moisture conditions and precipitation in different synoptic conditions has been performed by Findell and Eltahir (2003) using a regional atmospheric model and observations. To gain insight into the combined influence of soil moisture and wind, dry and wet soil experiments were performed. In addition, experiments were conducted where the wind magnitude of the initial conditions were decreased. The inclusion of three dimensional wind effects in the study of soil-moisture feedbacks proved to be very important and redefined the cases that favored or suppressed convection. It was found that low-level backing winds or unidirectional winds with strong vertical wind shear suppressed convection under both dry and wet soil moisture conditions. On the other hand, moderately veering winds below 300 mb enhanced convective development. These results suggested winds can exert a very important influence and control on the development of convective processes within the boundary layer.

However, to what extent and in what way the wind was modified by the soil moisture especially close to the surface is unknown. This question has been addressed only as a side issue in many of the above studies and just a few have looked at the effects of soil moisture on lower level wind. The latter was addressed from the perspective of air quality (Jacobson, 1999) and of uncertainty in initial conditions for regional ensemble forecasting (Sutton et al., 2006). It has been suggested that moderate changes in soil moisture bring about changes in the initiation and

location of convection which allow the required spread for short-range ensemble weather forecasts (Sutton et al., 2006).

In this context, the main objective of this case study was to demonstrate the sensitivity of the lower atmospheric energy partitioning represented by Bowen ratio, atmospheric stability, wind field, and precipitation to systematic changes in soil moisture for an area in western Kentucky. The MM5 and the Noah land surface scheme were used for this purpose. The model was applied for the entire month of June, 2006 to determine the sensitivity. To fulfill the objective of this study, observed (control) soil moisture content (volumetric, m^3 m^{-3}) was either decreased or increased systematically up to 0.15 with an interval of 0.05. This provided us with six anomalous soil moisture scenarios. The impacts of changes in soil moisture on the lower atmosphere were assessed for three precipitation events during June of 2006 controlled by three distinct synoptic conditions in the study area. This study is unique in a sense that it allowed us to understand interactions of various levels of soil moisture and their impacts on planetary boundary layer and precipitation under different types of synoptic conditions. It needs to be emphasized that the goal of this study was not to produce exact modeling of observed atmosphere rather to investigate its sensitivity built on reasonably reliable simulations (cf. Cheng and Cotton, 2004).

Kentucky was chosen as the center of the computational domain because of the particular ecological, physiographic, and climate region to which it belongs (Ulack et al., 1998; Kentucky Climate Center, 2008). A large number of studies related soil moisture and meso-scale atmospheric interactions were set in the Great Plains for justifiable reasons. Unlike Kentucky, the study locations for these research do not show significant within region variations. Kentucky is bounded by the Appalachian Mountains in the east and the Mississippi River on west while the east central part is characterized by rolling landscape while the western part resemble Midwestern region of the US. Western Part of the state is dominated by agricultural land use while fragmented forest is more common in the east. The study area is bordered by relatively drier midwestern region in the north and wetter southern region in the south. In other words, Kentucky is located in ecologically, physiographically, and climatically transitional zone. Hence, the experimental setting was unique and could enhance our understanding of mesoscale land surface atmosphere interactions under these such conditions.

Moreover, the authors of the present study are currently conducting research on odorous emissions from livestock waste lagoon and their mesoscale transport under variety of weather and seasonal conditions. This activity involves field measurement and coupling of chemistry and mesoscale models. Hence, the knowledge of soil moisture sensitivity is of great importance to understand modulation and behavior of boundary layer and for deriving the uncertainty in the transport and diffusion of pollutants from an ensemble of model outputs.

BACKGROUND

The soil-atmosphere feedback is thought to be one key element where soil moisture and a preconditioned atmosphere combine to inhibit or increase convection in

"direct" or "indirect" ways (Schar et al., 1999; Findell and Eltahir, 2003; Lawrence and Slingo, 2005). The direct pathway of this feedback is simply that of recycling the local atmospheric water content producing more precipitation at the expense of extra evaporation from the soil and the vegetation. This simple concept was in fact used in the late 1930s to increase rain by cutting down forests and opening areas susceptible to evaporation and larger runoff (Brubaker et al., 1993). The direct pathway was later contested and termed the "evapotranspiration-precipitation fallacy."

On the other hand, for the indirect pathway, atmospheric water, originating in the ocean or land, has residence times on the order of a week (Schar et al., 1999) and can be transported thousands of kilometers before it precipitates. Precipitation induces larger evapotranspiration producing a low Bowen ratio (since more energy is used to evaporate than to warm the soil). The result is shallower and moister boundary layers (e.g., Pielke, 2001). Since wetter surfaces have lower albedo, the soil absorbs more solar radiation and combined latent and sensible heat fluxes are larger than those over a drier soil (if we neglect soil heat flux). The moistening of the boundary layer and the energy flux increase are necessary conditions to make this layer unstable to vertical velocity perturbations and can precondition the atmosphere to generate moist convection subsequently leading to precipitation. Cloud cover could contribute to a negative feedback process. However, the reduction in net radiation absorbed by the wet surface under cloud cover can be compensated by the presence of water vapor which is an excellent greenhouse gas and may increase the longwave radiation towards the surface. This increases latent heat fluxes leading to further moistening of boundary layer (Schar et al., 1999; Pal and Eltahir, 2001).

The representation of the processes included in these soil-moisture precipitation feedbacks continues to be a matter of some controversy among atmospheric modelers at global and regional scales (Avissar and Liu, 1996; Giorgi et al., 1996; Koster et al., 2002; Lawrence and Slingo, 2005). Observational evidence in support of this feedback has come from a number of regional studies (Ek and Mahrt, 1994; Findell and Eltahir, 1997). For example, it was found that soil moisture status and its feedback through moist static energy influences occurrences of precipitation (Findell and Eltahir, 1997). Later, Findell and Eltahir (2003) found that the atmosphere-soil-moisture feedback depended on two parameters including the convective triggering potential (a measure of the temperature lapse rate between 1 and 3 km) and a low level humidity index. Combinations of these two parameters defined three types of early morning soundings where one favored precipitation over dry soils while the other, favored precipitation over wet soils. A third type, whose convective potential for generating rainfall was unchanged regardless of any combination. In summary, it was evident from the above studies that soil moisture plays a significant role in development of local precipitation events.

Moreover, it must be noted that earlier studies emphasized the thermodynamic aspect of atmospheric response to soil moisture conditions. This was natural since the main interest was in predicting precipitation under many different scenarios of atmosphere-soil interactions. To our knowledge, Jacobson (1999) was the only study that addressed the direct response in wind field to changes in soil moisture. In this study the main concern was the change in near surface wind field in the Los

Angeles basin and most of the response was basically due to the large sea–land het-
erogeneity.

   Here we studied the direct influence of soil moisture both on the response of
atmospheric thermodynamics and wind fields. For each of the experiments in this
study, soil moisture was changed uniformly over the entire domain. It was an impor-
tant feature of this study since we wanted to minimize the effects of horizontal gra-
dients in soil moisture conditions which are known to produce sea breeze-like
effects (Ookuchi et al., 1984).

EXPERIMENTAL DESIGN

   The MM5 regional atmospheric model version 3 was used in this study (http://
www.mmm.ucar.edu/mm5/mm5-home.html). The conservation equations for
mass, momentum, energy, and water are solved using a terrain following coordi-
nate system. The MM5 was designed to be coupled to a variety of physical modules.
The Noah land surface model (LSM; Chen and Dudhia, 2001) was chosen for rep-
resentation of land processes. The Noah LSM used four soil layers (10, 30, 60, and
100 cm) to predict soil temperature, soil water/ice, and snow cover. The total soil
depth was 2 m with the root zone in the upper 1 m of the soil. The quality of soil
moisture products from LSM depends critically on the accuracy of meteorological
data including precipitation. Although progress has been made in retrieving soil
moisture with remote sensing techniques and assimilation of observed data, uncer-
tainty in soil moisture remains an open problem not only globally but regionally
with very few observational sites in the world providing long-term data (Mahmood
and Hubbard, 2004).

   For the convection parameterization a version of the Kain-Fritsch scheme that
included shallow convection (Kain, 2004) was used. In addition, the MRF turbulent
scheme was adopted (Hong and Pan, 1996). Two two-way nested domains were
used over western Kentucky centered at 36.7°N latitude and 86.6°W longitude
(smaller box within domain 2) with the mother domain dimensions of 522 km by
592 km at 18 km horizontal resolution (domain 1; Fig. 1). The nested domain had
a horizontal resolution of 6 km and covered an area of 294 km by 186 km (domain
2; Fig. 1). Three early tests were conducted to establish the dependence of model
simulations on the vertical resolution. These included model simulations with 23,
31, and 38 vertical levels. It was found that simulations with 31 levels did not differ
substantially from those with 38 levels. However, the 23 level version of the model
run had significant differences in precipitation rates with the higher vertical resolu-
tion model simulations. Results reported here were from the 31 level resolution
simulation which had the top at 100 hPa, and 18 levels below the 0.65 sigma level.

   The horizontal resolution of the nested domain was quite close to the limits of
validity of the cumulus parameterizations. It was considered necessary to use the
Kain-Fritsch for the nested domain since experiments without convective
parameterizations did not produce precipitation patterns sufficiently close to
observed. It was expected that some of our estimates would be sensitive to the
selection of cumulus parameterizations. However, it will be shown in the subse-
quent sections that there is confidence in the results and the model was able to
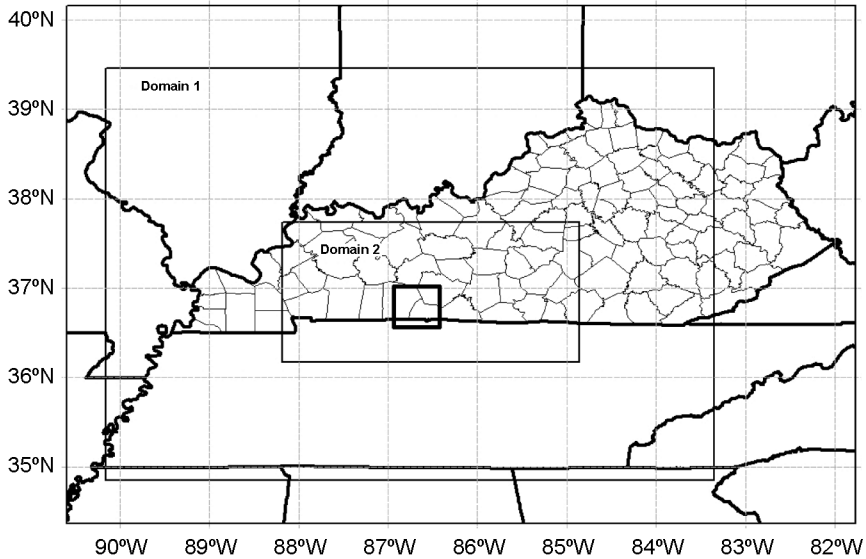
Fig. 1. Outer and nested domains. The small box within Kentucky is representative of physiographic properties of domain 1 and 2.

capture the majority of convective events within the study period and produced values of precipitation not far from those observed. The North American Regional Reanalysis (NARR) was used to verify the model simulated precipitation. It contained analyses of precipitation derived from several sources (Mesinger et al., 2006) at 32 km resolution.

The Noah LSM was initialized using the USGS high spatial resolution data provided on the MM5 web site. The database included 24 land use categories and high resolution terrain data. To initialize MM5 the NCEP Final Analyses (FNL) at 1° × 1° resolution was used for the entire month of June 2006. This month was selected partly because of the availability of data. It also contained three types of synoptic meteorological conditions corresponding to weak, moderate, and strong forcing as evidenced from observed surface wind conditions. This study was concerned with planetary boundary layer conditions including Bowen ratio, stability, wind field, and precipitation under these conditions and their changes due to soil moisture variations. In addition to the meteorological data required to initialize the atmospheric model, the FNL analyses contained soil moisture and temperature data produced also by a version of the Noah LSM. These soil variables were also given at the same levels required by the Noah LSM of the MM5 simulation. A control simulation was performed starting June 1, 2006 without spin-up time forced at its lateral walls with FNL analyses data updated every 6 hours. Since the objective of the present study was to estimate the influence of soil moisture on the near-surface and planetary boundary layer fields, it was considered that a long spin-up time of a year as is customary with the Noah LSM (Grunmann, 2005) would not reveal more than a "warm start" experiment. If our only intention was to isolate the effects of moisture

changes in their pure form, we faced an inherent difficulty in producing a clean cut experiment in a regional atmospheric model coupled to its LSM. We must remember that the MM5 was forced at its lateral walls with the analysis fields which have information of land–surface processes and therefore contains already a measure of a hydrological balance. Under these conditions, if we were to perturb the soil moisture for a period of several months, the atmospheric model would return to its equilibrium condition within 6 to 18 months depending on the initial state of the soil moisture and the atmosphere (Grunmann, 2005). For this reason we decided to perturb the soil moisture for a period of one month which is several orders of magnitude smaller than the 6 or 18 months e-folding time of the model equilibration. Therefore, it was not the aim of the present study to achieve long-term climatological equilibrium between the model atmosphere and the coupled LSM, but rather to look at the effect of perturbing the soil moisture for a period, long enough to have some reasonable representation of the actual observed data and to leave an imprint on the atmosphere. To that end, anomaly experiments in soil moisture were prepared from the model interpolated initial conditions while the meteorological initial conditions were left intact. Six sets of experiments (sensitivity tests) were performed with the soil moisture decreased (and increased) with respect to the volumetric moisture control values by 0.05, 0.10, and 0.15 uniformly everywhere in the mother and nested domain and at *all four* subsurface levels. Accordingly, these were designated as DE05, DE10, and DE15 for the dry experiments and WE05, WE10, and WE15 for the wet experiments. This uniform change in volumetric soil moisture was chosen so as to maintain the horizontal and vertical gradients of moisture. The magnitude of the soil moisture change with respect to the amount of precipitation received in June 2006 was compared. In the DE15, the water deficit amounted to 15 cm in a 1 m soil column of the root zone. These water deficits could not be removed with the observed accumulated precipitation of 3 cm for entire June 2006 for the inner model domain from NARR data.

Ordinarily, researchers (e.g., Schar et al., 1999; Aligo et al., 2007) would multiply soil moisture values by one single factor larger (smaller) than unity with the effect of increasing (decreasing) both horizontal and vertical gradients in soil moisture. This could induce mesoscale circulations adding one more complication to the interpretation of model results (Ookuchi et al., 1984). For this reason it was decided to simply sum or subtract a constant value from the original soil moisture values fed to the control run at the end of the interpolation process that produces the initial and boundary conditions for the MM5 (Chen and Dudhia, 2001).

The Noah LSM internally generated the soil field capacity values and its wilting point and calculated values of soil moisture depending on land use. Thus, soil moisture can exceed its field capacity after rain and relax later on. The e-folding time of this relaxation process depends on the state of the initial soil moisture, land use, and vegetation cover. As mentioned above, the Noah LSM uses the 25 category USGS land use values with a spatial resolution of 30 seconds (about 1 km) which are later interpolated to the model's grid.

The model's computational nested domain land category corresponded to silt loam, which has a prescribed wilting point of 0.084 (m^3 m^{-3}) and a reference field capacity of 0.360 (m^3 m^{-3}; Table 2 in Chen and Dudhia, 2001). The dominant

vegetation cover for this region was represented by crop and woodland. Except for the case of horizontal maps of synoptic conditions and precipitation presented in the next two sections, the results for the different experiments reported here, referred to an area within the state of Kentucky close to the Tennessee border centered about 36.7°N latitude and 86.7°W longitude (see smallest box in Fig. 1). Land surface properties of this area were representative of the larger region within domain 1 and 2.

SYNOPTIC CONDITIONS FOR JUNE 2006

The synoptic conditions that characterized the June 2006 were typical of this time of the year with frontal systems frequently crossing the state of Kentucky. From June 1 through 4, a very well developed eastbound front passing through a large area of the Central Plains produced a large amount of rainfall (synoptic map not shown). Figure 2 shows the mean sea level surface pressure and wind fields from the NARR for June 12, June 18–19, and June 23 at 0000Z for the Central and Eastern United States. Left and right panels of Figure 3 show precipitation from NARR data and control runs, respectively. These two sets of figures are used concurrently during following discussion.

The precipitation of June 12 was caused by a frontal disturbance that evolved into an occluded front and produced significant precipitation over central Kentucky (Fig. 3A). At this time, a weak low pressure system remained stationary over Kentucky with westerly winds in the south and northeasterly winds over the northeastern region. Wind speed varied from calm to about 8 m s^{-1} (Fig. 2A). Following this event, a persistent high pressure system kept the region dry for next six days until June 18 when a new precipitation event was observed. A cold front and moisture advection from the Gulf of Mexico created unstable conditions and produced significant amounts of precipitation over southwestern Kentucky and the northwestern Tennessee regions (Fig. 3B). On June 19, another precipitation event occurred with somewhat similar characteristics of moisture transport from the Gulf of Mexico and wind fields (Fig. 3C). Data indicated surface wind speeds were of the order of 10 m s^{-1} or larger (Figs. 2B–2C) for June 18 and June 19. In addition, a precipitation event in Central Kentucky was observed on June 23 (Fig. 3D). This was produced by a cold front and some moisture advection from the Gulf of Mexico. The wind speed observed during this event ranged from calm to about 5 m s^{-1} (Fig. 2D). A few additional events occurred during the last days of June with lesser amounts of precipitation (not shown). Thus, it was possible to define the June 18–19 precipitation events as strongly influenced by the synoptic-scale setting. On the other hand, the June 12 and June 23 episodes were moderately and weakly influenced by synoptic conditions, respectively. Hence, convective activities were affected differently during each of these events.

RESULTS AND DISCUSSION

Simulated Precipitation

Figures 3A and 3E show the 12-hour accumulated precipitation from June 11, 1800 Z, to June 12, 0600 Z, centered at June 12, 0000 Z, from the CTRL simulation
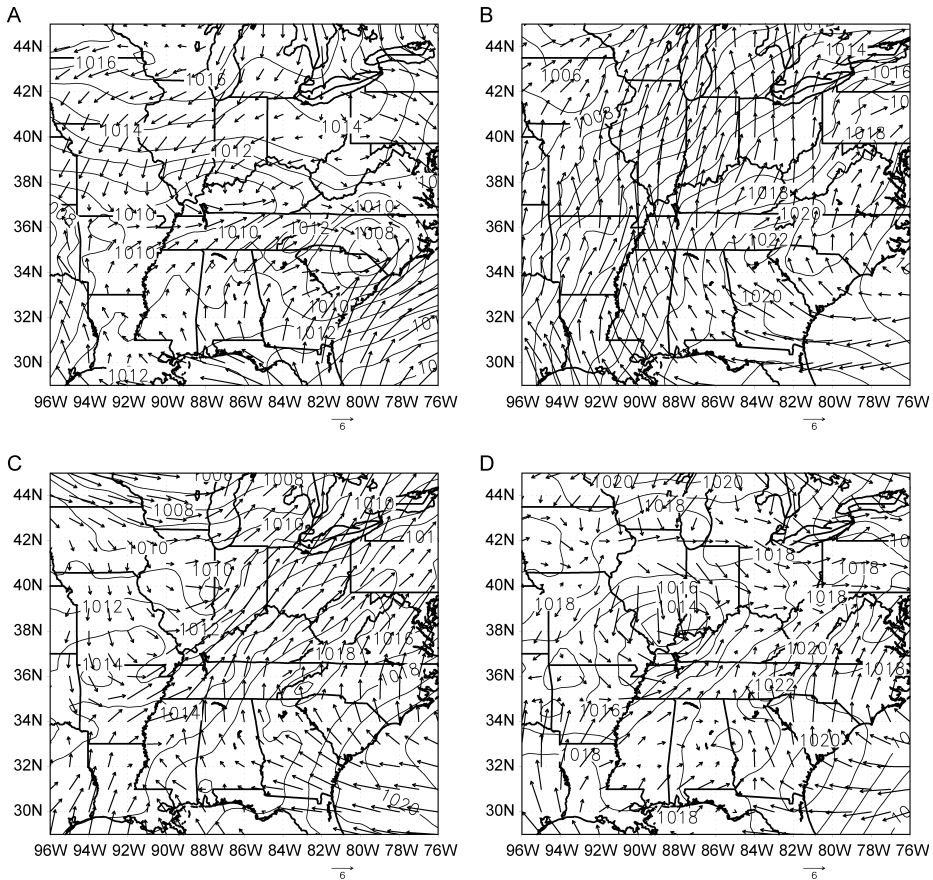
Fig. 2. Mean sea level pressure (mb) and surface wind field (m s^{-1}) for (A) June 12, 0000 Z, (B) June 18, 0000 Z, (C) June 19, 0000 Z, and (D) June 23, 0000 Z from the North American Regional Reanalysis.

in the mother domain and from the available NARR data. The simulation for June 12 showed two maxima in precipitation while the observational data showed only one maximum at the center of the state. The CTRL simulated precipitation tended to over-estimate at these two places due to this particular simulated horizontal precipitation distribution perhaps due to a much higher spatial resolution in the model. The 12 hour accumulated precipitation centered at June 18, 0000 Z (Figs. 3B and 3F) showed substantial differences in spatial distribution and magnitude of precipitation for the simulation and the observational data. Nonetheless, a maximum in precipitation in the southwest corner of Kentucky and northwest of Tennessee was well placed in the simulation. The simulated precipitation amount also agreed fairly well with that observed. On the other hand, the model overestimated precipitation over northwest-ern Kentucky and southern Ohio. Figures 3C and 3G show NARR and CTRL the 12 hour accumulated precipitation, respectively, centered at June 19 0000 Z. The CTRL simulation captured the general horizontal distribution of precipitation but tended to
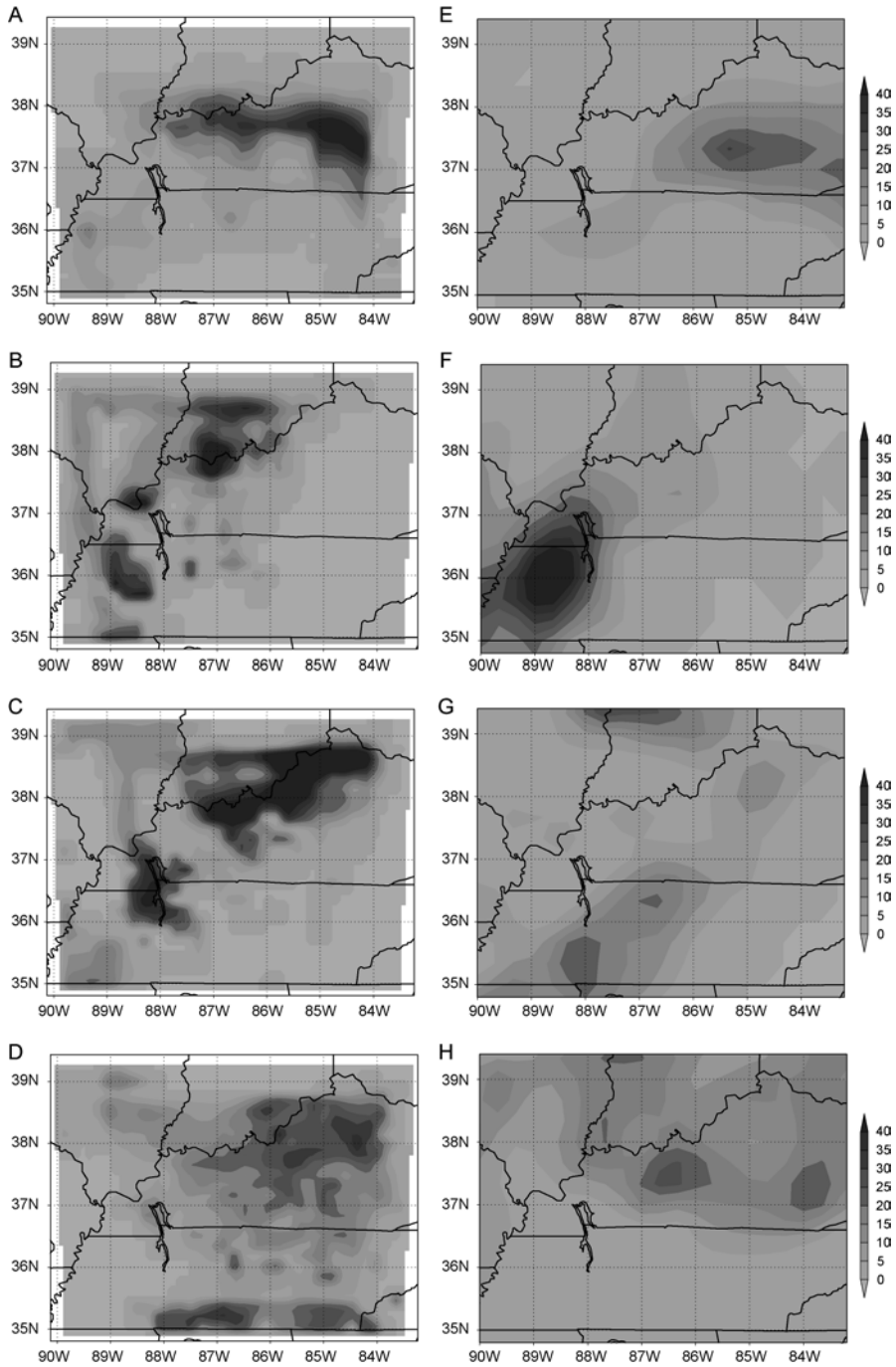
Fig. 3. Twelve-hour accumulated precipitation (mm) for the control run (A and C) and the NARR observational data (B and D) centered on June 12 0000 Z (A and B), centered on June 18, 0000 Z (C and D), centered on June 19, 0000 Z (E and F), and centered on June 23, 0000 Z (G and H) for the outer domain.

overestimate observed values. Finally for the 12 hour accumulated precipitation centered at June 23 0000 Z (Figs. 3D and 3H) the CTRL simulation agreed in general with the spatial distribution of observed precipitation although it tended to underestimate the observed maxima in Central Kentucky. We note that increase of domain size does not necessarily remove the impact of the model lateral boundaries ("edge effect"). During this study, a number of simulations were conducted with a 12 km horizontal resolution (not shown) covering a large portion of the Eastern US centered on Kentucky. The results suggested that the accumulated precipitation to be spatially similar to the one shown here. However, at times, significant differences in timing of precipitation were found between 12 km simulations with larger domain and NARR data and control simulations. It was also evident that our simulations with the domain size used in this study provided superior estimates of precipitation at both spatial and temporal scales compared to the larger domain with 12 km simulations. As a result, we adopted the current domain size shown in Figure 1.

*Impacts of Drier than "Observed" Soil Moisture Content*

Figures 4A–4C show the precipitation rates for the dry soil moisture experiments and the control simulation for each of these periods. During June 12, the CTRL simulated maximum precipitation rates of about 3 mm 3 hr^{-1} compared to about 8 mm 3 hr^{-1} in the NARR data (Fig. 4A). Correspondingly, the precipitation rates for the DE05, DE10 and DE15 showed increasingly larger precipitation rates compared to the control experiment (up to 5 mm in 3 hr) as the soil volumetric fraction was decreased with respect to the control simulation.

Figure 4B shows the precipitation rates for the June 18–19 event. During CTRL runs, with the exception of one small peak (June 18, 1200 Z), the precipitation events of June 18 and 19 are reasonably well simulated in both magnitude and timing. For DE05 and DE10 experiments the second observed precipitation peak of June 18 2200 Z (13.5 mm hr^{-1}) are almost indistinguishable in both amplitude and timing and just slightly larger (less than 1 mm 3 h^{-1}) in amplitude from the CTRL run. On the other hand, the DE15 caused notable differences for this date with the other dry experiments and the CTRL run. It was found that DE15 had a peak amplitude of about 3.5 mm 3 h^{-1} centered near June 18, 2200 Z.

For June 23, modeled CTRL precipitation values differed from NARR observations. NARR data shows 4 peaks of precipitation with amplitudes between 1 and 3 mm 3 h^{-1} (Fig. 4C). Note that near June 0600 Z for one precipitation peak, compared to NARR data, the CTRL simulation overestimated the observed values by almost a factor of 4 (10.5 mm 3 h^{-1}; Fig. 4C). It was found that precipitation amplitudes decreased for DE05, DE10, and DE15 experiments (Fig. 4E). On June 23, peak precipitation amplitudes were at 7.5, 8.5, and 3.9 mm 3 h^{-1} for DE05, DE10, and DE15, respectively.

Impact of Wetter than "Observed" Soil Moisture Content

Wet experiments (WE05, WE10, and WE15) for June 12 were very similar to the CTRL run with less than a 1 mm 3 h^{-1} precipitation differences (Fig. 4D). It was
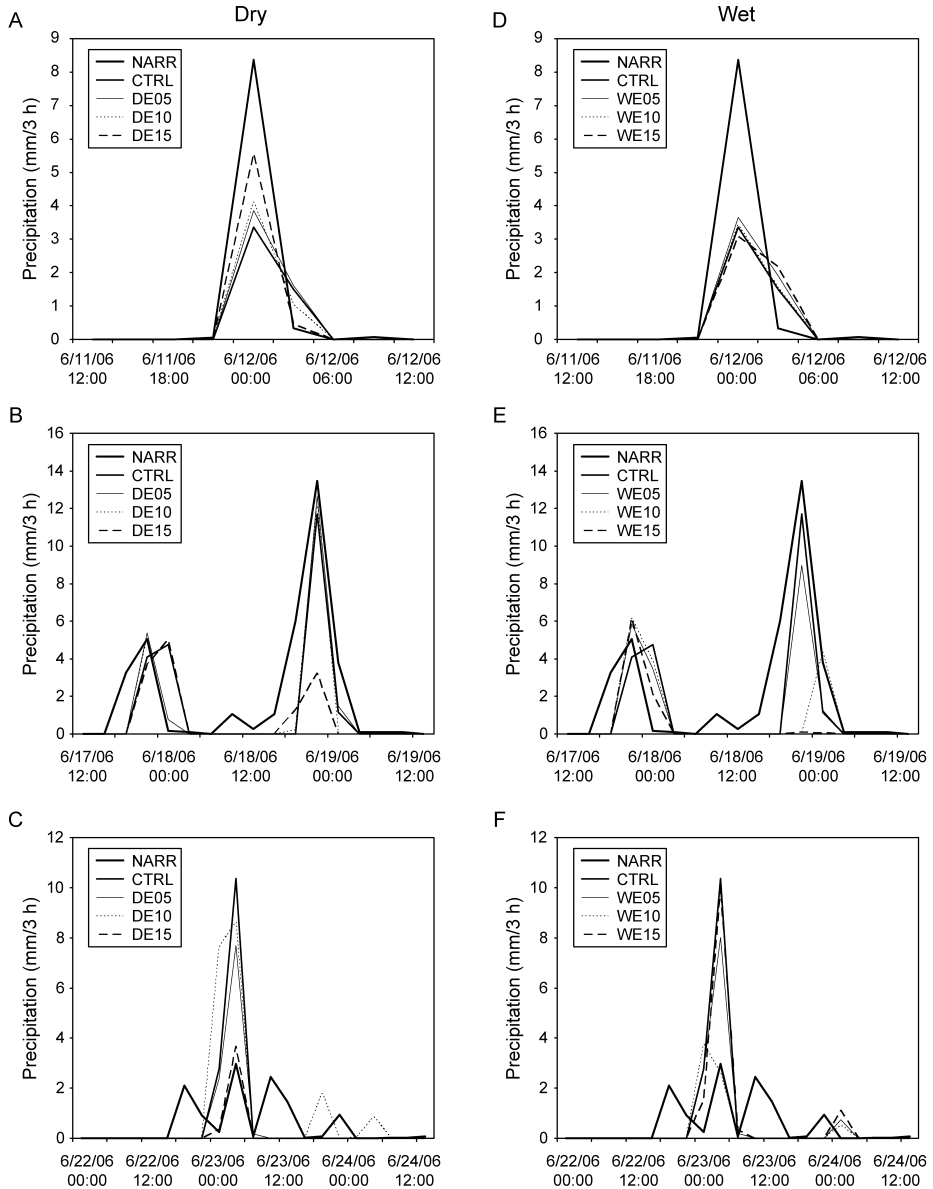
Fig. 4. Area averaged time series of accumulated precipitation (mm 3 h^{-1}) near (36.7°N, 86.7°W) for the events of June 12 (A and D), June 18–19 (B and E), and June 23 (C and F). Left and right panels include simulations from the dry and wet experiments, respectively.

found that with increasing soil moisture, precipitation did not increase linearly. Soil was wet for CTRL simulations and hence, systematic increase of soil moisture compared to CTRL did not cause significant changes in planetary boundary layer characteristics. During June 18, wet soils resulted in higher precipitation (Fig. 4E). On

the other hand, during June 19, a progressive reduction in amplitudes of precipitation from 8.7, 4.0, and to about 0.1 mm 3 h^{-1} occurred for WE05, WE10, and WE15 experiments, respectively (Fig. 4E). The precipitation evolution for the June 18–19 event for the wet anomaly simulation indicated a larger suppression in precipitation than its dry counterpart during the second peak (on June 19) event. However, it went against an expected increase in precipitation for wetter soils. The potential cause for this type of outcome is discussed above.

Subsequently, we examined the period for June 23 (Fig. 4F). At June 23, 0600 Z, peak precipitation for WE05, WE10, and WE15 are 8 mm 3 h^{-1}, 3.9 mm 3 h^{-1}, and 10.5 mm 3 h^{-1}, respectively. The latter value is slightly smaller than the CTRL precipitation value. In summary, changes in precipitation rate in response to systematic modifications in soil moisture are not linear. It was also found that impact of soil moisture forcing on atmosphere partly depends on the prevailing synoptic state. This suggests complex land–atmosphere interactions under variety of soil moisture status and existing state of the atmosphere.

Bowen Ratio and Precipitation Under Dry and Wet Soil Conditions

In this and following section, the discussion is centered on the differences between the CTRL simulation and the two anomaly experiments, namely DE15 and WE15. These two experiments were chosen in view of the response in precipitation, presented in the previous section, which in most cases differed notably in intensity from the rest of the dry and wet experiments.

To determine a possible link between the observed precipitation behavior and the state of the soil moisture, the Bowen ratio and precipitation rates are presented together in Figure 5. Figure 5A shows the Bowen ratio (unbroken lines) and the precipitation (dashed lines) for June 12 (figure also includes June 11). Near noon local time on June 11, the Bowen ratio values for the CTRL and the WE15 were very similar. On the other hand, the DE15 had a larger value since sensible heat fluxes (latent heat fluxes) peak at this time of the day and they were larger (smaller) than the corresponding fluxes in the CTRL simulation. About three hours later (1800 Z) the Bowen ratio values began decreasing for the CTRL, the DE15 and WE15 experiments. As they continued to decrease the precipitation rates grew to a maximum at 0000 Z of June 12. Subsequently, at about 0600 Z of June 12 precipitation ceased in all experiments and the Bowen ratio starts to increase as the diurnal cycle onsets again. The large peaks of Bowen ratio in the CTRL simulation were due to large sensible and small latent heat fluxes.

The Bowen ratio for the June 18–19 and the June 23 events for dry and wet experiments are presented in Figures 5B and 5C. The behavior was similar in the sense that a very small Bowen ratio was always observed when precipitation began in both dry and wet soil experiments. It has been shown that a small Bowen ratio is necessary but not suffcient to generate deep cumulus convection (Segal et al., 1995; Pal and Eltahir, 2001). At this point, however, comparison between the Bowen ratio and precipitation rates for the different experiments did not reveal a clear relationship between these two quantities.
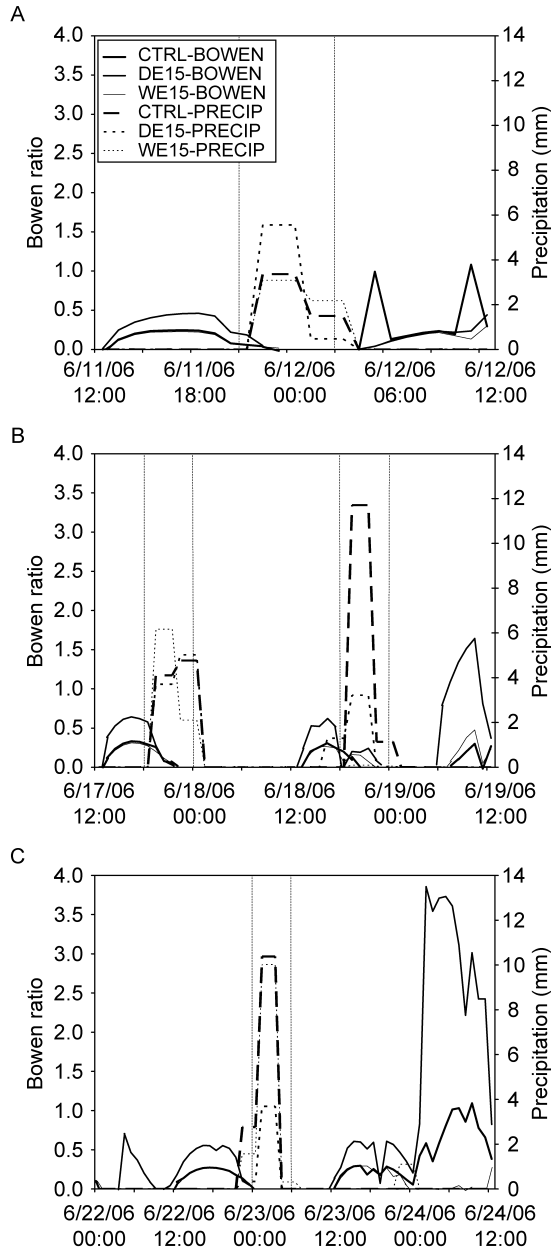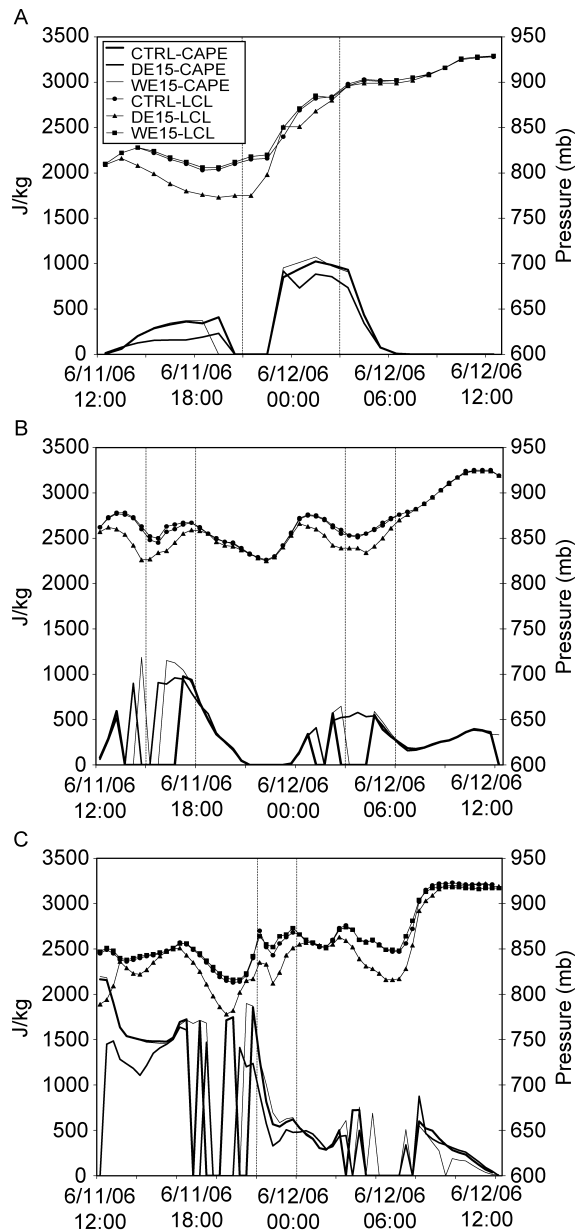
Fig. 5. Time series of Bowen ratio and precipitation for (A) June 12, (B) June 18–19, and (C) June 23.

Atmospheric Stability Under Dry and Wet Soil Conditions: LCL and CAPE

Figure 6 shows the lifting condensation level (LCL) and the convective available potential energy (CAPE). The time intervals of the precipitation events discussed in

QUINTANAR ET AL.

Fig. 6. Time series of convective available potential energy (J kg^{-1}) and lifting condensation level (LCL; mb).

the precedent section are marked in Figure 6 to aid the comparison with precipitation in Figure 5. It was found that the LCL of the CTRL and that of WE15 experiments were almost equal. On the other hand, the LCL of the DE15 was located at higher altitude than those of the CTRL and the WE15 experiments. This behavior

can be explained from the results for the Bowen ratio in the previous section. As Bowen ratio increased for drier soils (Fig. 5), moisture availability to air parcels near the surface was restricted. Hence, drier air parcels needed to be lifted to higher altitude (lower pressure level) before they can form clouds. As a result, model simulation calculated a higher LCL (lower pressure level) for DE15. Opposite forcing caused lower LCL heights for moist soils (cf. Schrieber et al., 1996).

Besides being a measure of buoyancy, CAPE is also a measure of maximum vertical motion and can thus account as a possible lifting mechanism for deep convection. During the June 12 event between June 11 2100 Z and June 12 0300 Z (see marks on Fig. 6A), the LCL was initially located close to 775 mb in the DE15 experiment. On the other hand, for the CTRL and the WE15 experiments, a LCL was located near 800 mb. This was consistent with the fact that at lower levels the CTRL and the WE15 simulations had moister atmospheres than the DE15. On June 12, 0000 Z, the LCL of the CTRL and the WE15 experiments were about 200 m (about 20 mb larger) below the LCL corresponding to the DE15 run. After June 12, 0300 Z the LCL was almost identical in all simulations. At this time, CAPE values for the CTRL and the WE15 were between 100 and 200 J kg^{-1} larger than the corresponding values for the DE15 experiment. However, precipitation rates for the DE15 experiment were larger than the CTRL and WE15 experiments as shown in the previous section (Fig. 5A).

Figures 6B and 6C present the corresponding LCL and CAPE values for the June 18–19 and June 23 events, respectively. It was found that between the intervals marked in Figure 6B and 6C the LCL of the DE15 was always located above those of the CTRL and WE15 simulations indicating greater possibility of deeper convection in these last two simulations. For the first marked interval in the June 18–19 event the largest CAPE corresponded to the WE15 experiment which also showed a slightly larger precipitation rate (1.75 mm 3 h^{-1}) when compared to the CTRL and the DE15 runs (1.4 mm 3 h^{-1}). CAPE values for the CTRL and the WE15 were generally similar at this time.

The second segment in Figure 6B was more difficult to interpret since CAPE values for the CTRL and the WE15 experiments collapsed at the time of maximum precipitation rates (Fig. 5B). Finally, the June 23 event showed values of CAPE larger than that of about 1800 J kg^{-1} that had been seen previous to the precipitation event in all experiments (Fig. 6C). For the marked time interval, during precipitation events, CAPE values decreased rapidly at the same rate with the CTRL and WE15. At this time, precipitation rates were 3 times larger in the CTRL and the WE15 experiments compared to the DE15 run.

It needs to be noted that CAPE responded to the degree of synoptic forcing. The smaller values of CAPE, before and during the precipitation events occurred during the strong synoptic forcing (June 18–19) while the largest occurred during the weaker event (June 23). Nevertheless, these results showed that the precipitation rate differences between simulations could not be directly related to the change in stability of the model atmosphere in the different anomalous soil moisture experiments. Lower LCL in height should produce deeper convection. However, as seen in Figure 5A, this did not necessarily result in larger precipitation rates in the wet experiment or less precipitation in the dry simulation.

Equivalent Potential Temperature

Here we analyzed stability by using equivalent potential temperature (θ_e) as a proxy for moist static energy (Pielke, 2001). Figures 7A–7F show this quantity as a function of sigma vertical levels and time for the events of June 12, June 18–19, and June 23. The time evolution of θ_e clearly showed the changes in planetary boundary layer height before, after, and during the precipitation events. The boundary layer depths for CTRL and WE15 were very similar. On the other hand, slightly greater depth for the DE15 experiment could be linked to a larger Bowen ratio at about the time of precipitation (not shown).

The θ_e difference between the CTRL and DE15 as well as CTRL and WE15 was calculated for an analysis of the atmospheric stability. On June 12 at lower levels, when compared to DE15, the CTRL simulations showed up to 4 K higher and lower θ_e before and after the precipitation event, respectively (Fig. 7A). A similar comparison between CTRL and the WE15 simulations showed the opposite result (Fig. 7B). It is interesting to note, at this point, that θ_e provided a more sensitive index to the changes in precipitation (or lack of thereof) when comparing the CTRL and the anomaly experiments.

The second peak of June 18–19 event at 1800 Z showed a marked difference (up to 4 K) in θ_e between the CTRL and the DE15 simulations (Fig. 7C). This partially explained why the CTRL simulation has more possibility of larger precipitation rates than the DE15 at this time. The comparison between the CTRL and the WE15 at the onset of precipitation suggested 2 K larger value of θ_e in the CTRL simulation at lower levels (Fig. 7D). For June 23 at 0000 Z, again, the differences between the CTRL and the DE15 and WE15 experiments are about 6 and 1 K higher and lower, respectively. Hence, we suggest that due to the moist prevailing land surface condition (not shown), the difference between CTRL and WE15 is small.

In summary, a low Bowen ratio was a necessary but not sufficient condition to establish convection and this condition alone did not necessarily lead to rainfall. Also, the LCL and CAPE were not good indicators of precipitation changes for the dry and wet soil moisture experiments. When the distributions of θ_e were examined, a clearer picture emerged which showed that θ_e was more sensitive to soil wetness. Subsequently, it is a reasonable indicator of precipitation changes under the dry and wet soil moisture conditions.

Modeled 3-D Wind Effects for Dry and Wet Soil Conditions

Vertical (cm s^{-1}) and horizontal velocity fields (20 m s^{-1} vector scale) are shown in Figure 8 for the three events of June 12, 18–19, and 23 as a function of height (upper, middle, and lower panels, respectively) under DE15 and WE15 soil moisture conditions. In addition, Figure 9 show differences between CTRL and DE15 and between CTRL and WE15. The following assessment would refer to these figures depicting results from the simulations and differences between CTRL and dry and wet experiments side-by-side.

From Figure 8, it was apparent that, for CTRL, DE15, and WE15, the vertical velocity was weaker during the June 18–19 episode when the synoptic forcing was
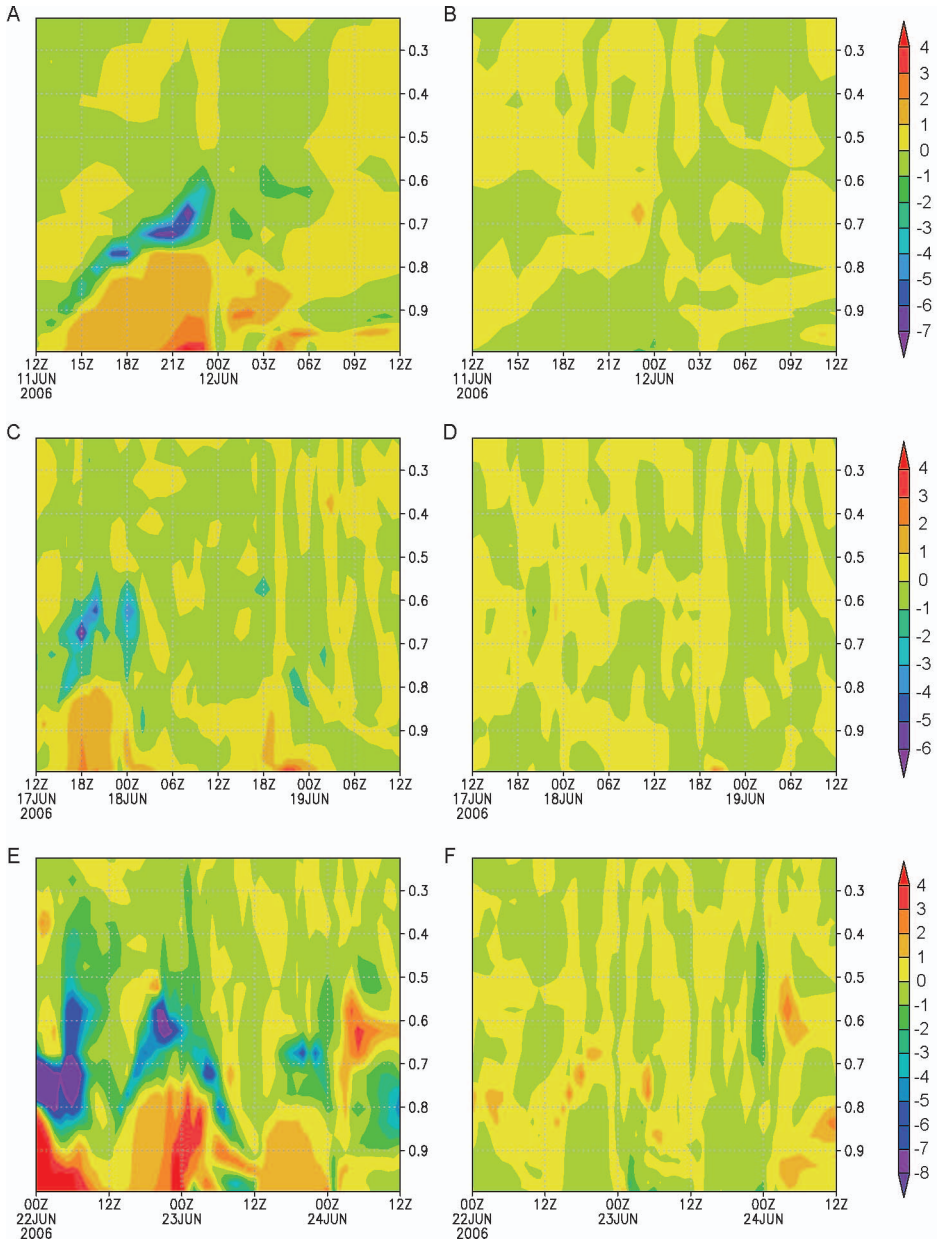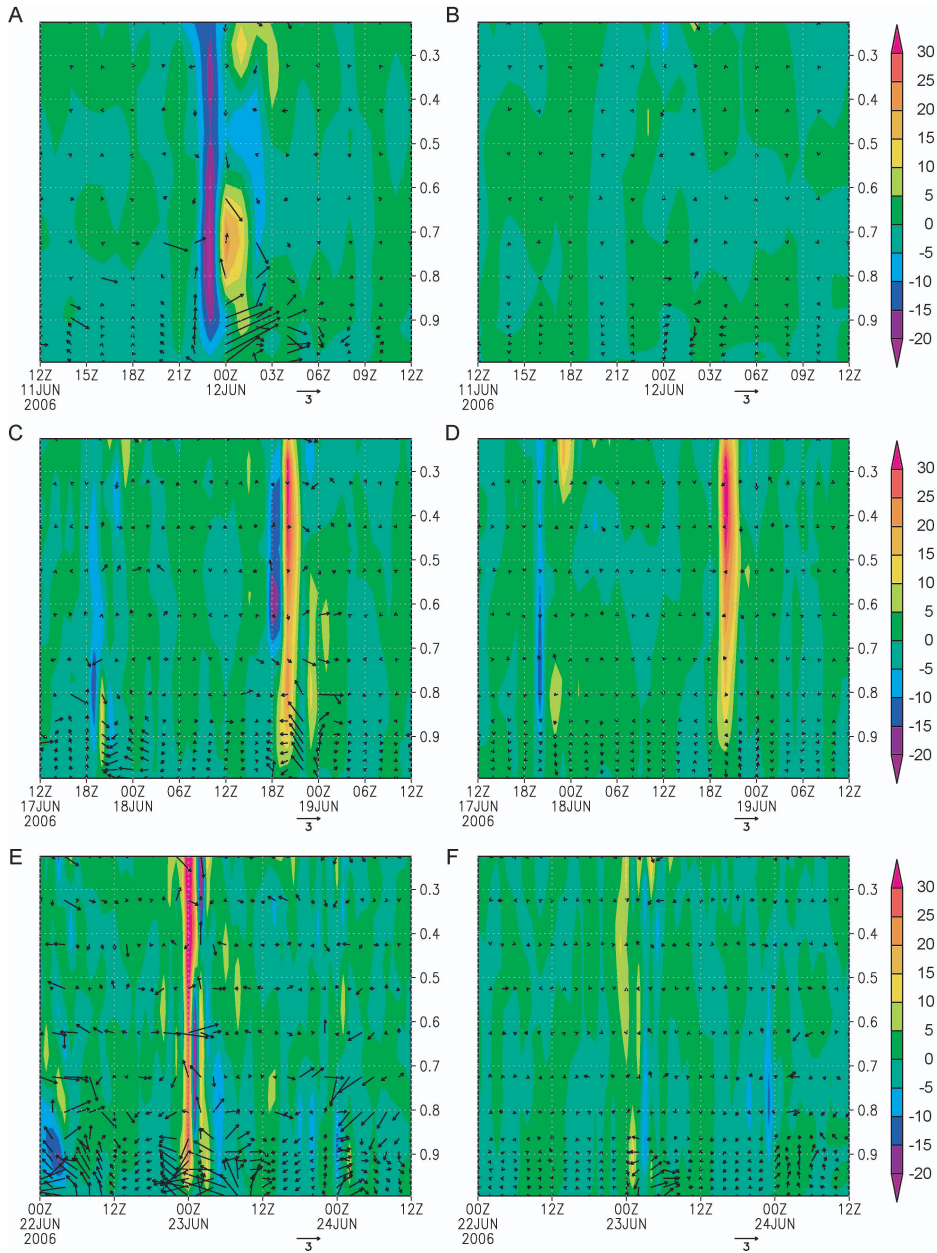
Fig. 7. Time versus sigma vertical coordinates cross sections of equivalent potential temperature (θ_e) for the CTRL minus DE15 (left panels) and the CTRL minus WE15 (right panels) for June 12 (A and B), for June 18–19 (C and D), and for June 23 (E and F).

stronger at all levels. On the other hand, the June 12 and June 23 events showed stronger vertical velocity under moderate and weak synoptic forcing settings that occurred on these respective dates. Figures 8A–8C show the corresponding vertical

QUINTANAR ET AL.
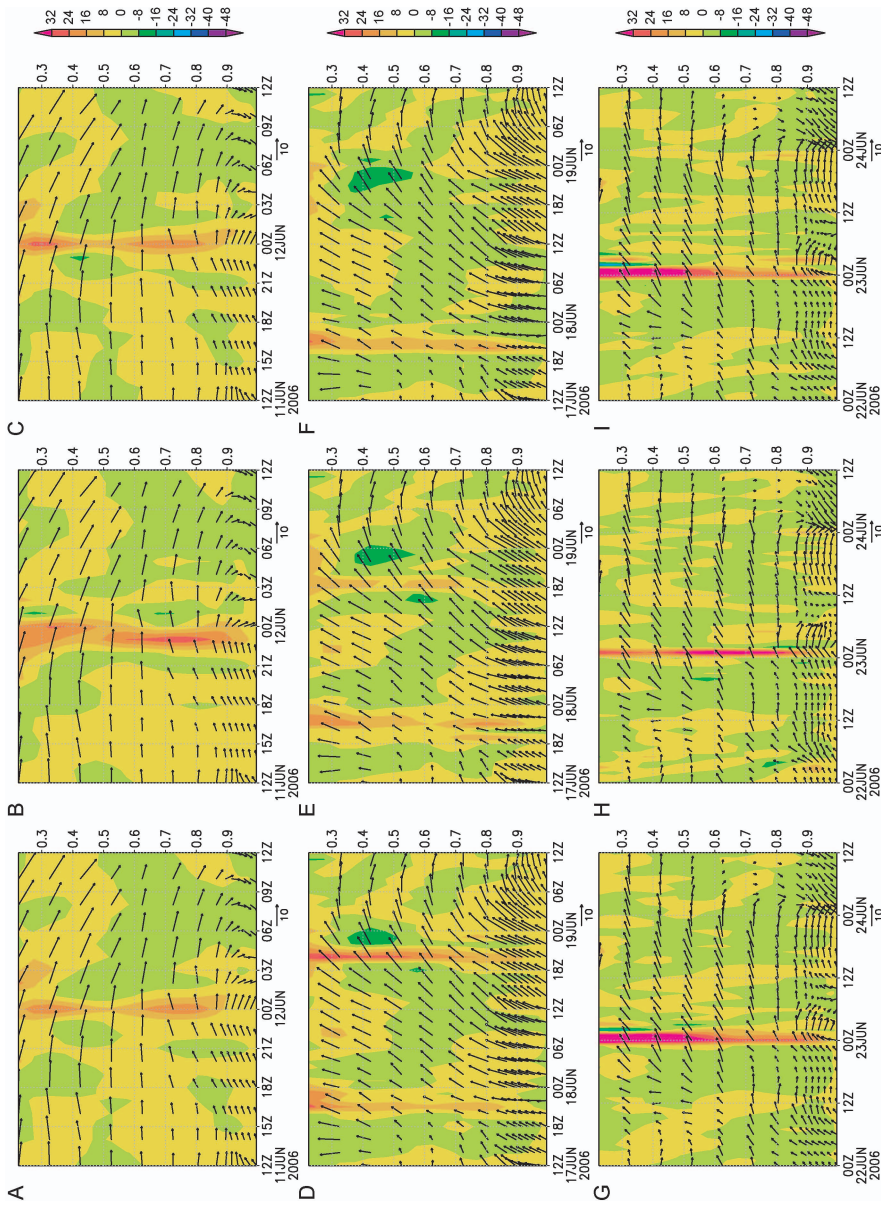
Fig. 8. Time versus sigma vertical coordinates cross-sections of the vertical wind velocity (cm s^{-1}) and the horizontal wind vector (m s^{-1}) for the CTRL run (left panels), DE15 (middle panels), WE15 (right panels) for June 12 (A, B, and C), June 18–19 (D, E, and F), and June 23 (G, H, and I).

Fig. 9. Time versus sigma vertical coordinates cross sections of vertical velocity (cm s^{-1}) and the horizontal wind vector (m s^{-1}) for the CTRL minus DE15 (left panels) and CTRL minus WE15 (right panels) for June 12 (A and B), for June 18–19 (C and D), and for June 23 (E and F).

and horizontal wind vectors for CTRL, DE15, and W15 experiments, respectively, for June 12 as function of sigma levels and time. The maximum vertical velocity

(about 40 cm s^{-1}) was found in the DE15 simulation which corresponds to the higher precipitation rates of June 12 (Fig. 6A). In all June 12 experiments, the horizontal wind vectors exhibited some degree of counterclockwise rotation as a function of height (backing) particularly after the deep cumulus convection had ceased. In Figure 8B it is clear how deeper convection started about 2 hours earlier in the DE15 run than in the CTRL and WE15 experiments. Hence at 0000Z of June 12 we expected to find a major difference in the horizontal wind components due to this time shift of deep convection.

Figures 8D–8F show wind fields for the June 18–19 event for CTRL, DE15, and WE15, respectively. Here we found that horizontal vector wind fields were of larger magnitude than the June 12 case and little or no appreciable rotation with height was detected during the precipitation events for all experiments. The unidirectional wind field was associated with a strong synoptic forcing and a suppression of convection. Vertical velocities for this event were smaller in than the June 12 or June 23 events. We suggest, however, that vertical velocity for the different experiments corresponded to the magnitude of the simulated precipitation rates (Fig. 6B).

Finally, the June 23 case is shown in Figures 8G–8I. Here, in contrast to the June 12 case the horizontal wind vector rotated clockwise with height (veering). This is a condition associated with warm advection and which adds buoyancy to parcels. It was also found that the veering was more pronounced for June 23 event in both dry and wet soil experiments. Again, the magnitude of vertical velocity corresponded to the precipitation rates found earlier (Fig. 6C) for this event.

The differences in CTRL-DE15 vertical and horizontal velocity (cm s^{-1}) for June 12 are presented in Figure 9A. A dipole pattern was evident at 0000 Z when the precipitation event occurred. This indicated that the drying of the soil resulted in early appearance of deep cumulus convection. The magnitude of the wind vector differences could be of the order of 8 to 10 m s^{-1} during the convective stage.

As expected, the CTRL-DE15 showed greater differences in vertical and horizontal wind vector velocity compared to the CTRL-WE15 simulations for June 12 (Figs. 9A–9B). A significant difference in the horizontal wind field was also apparent for CTRL-DE15 of up to 6 m s^{-1} in magnitude. For June 18–19 simulations, the CTRL-DE15 experiment indicated a dipole pattern at 1800 Z of June 18 and this corresponded to the second maximum in vertical wind velocity (Fig. 9C). For CTRL-WE15, the vertical velocity also showed notable differences in the second peak (Fig. 9D). This was expected since vertical velocity was suppressed in the WE15, which also resulted in no precipitation (Figs. 8F and 4D).

For the June 23 episode, differences in vertical velocity for CTRL-DE15 and CTRL-WE15 conditions were reflected in the dipole structures of Figures 9E and 9F, respectively. However, the vertical velocity maximum appeared to be delayed in the DE15 experiment compared to the CTRL simulation. The horizontal wind vectors showed significant differences between the CTRL and the DE15 with magnitudes reaching up to 6 m s^{-1}. The difference in CTRL-WE15 suggested that the windfield response was relatively muted for WE15 compared to DE15.

In summary, we found that vertical velocity was a useful index for simulated precipitation rates. However, this was not entirely surprising because the criteria to

generate precipitation in the current Kain-Fritsch parameterization scheme depends critically on the vertical velocities resolved by the model (Kain, 2004).

FINAL REMARKS

This study conducted a sensitivity assessment with the MM5 coupled to the Noah land surface model in which the initial soil moisture conditions were changed systematically to understand the response of planetary boundary layer and precipitation. The simulations were conducted for the entire month of June of 2006 and three precipitation events were analyzed. These precipitation events were influenced by distinct weak, moderate, and strong synoptic forcing. Hence, they allowed us to investigate interactions of variety of soil moisture state and their inter- actions with variable synoptic setting. It was found that soil moisture control on pre- cipitation can be well-explained via analysis of vertical velocity and θ_e. These atmospheric variables can be useful in determining soil moisture and precipitation linkages. In addition, small Bowen ratio was necessary but not in itself sufficient to trigger precipitation. This study suggests that LCL and CAPE were not as useful as vertical velocity and equivalent potential temperature in indicating precipitation development.

It was found that strong veering favored convection while lack of it suppressed precipitation, in agreement with earlier studies (Findell and Eltahir, 2003). Most importantly, such veering was very sensitive to the specification of soil moisture. This study reports that the magnitude of changes in the horizontal wind fields could be up to 10 m s^{-1} in extremely dry cases while experiments with more modest changes in soil moisture could produce changes in the order of 2 or 3 m s^{-1}. It was also found that θ_e was noticeably higher (up to 350 K) during precipitation events under weak synoptic condition. Moreover, compared to moderate and strong synoptic forcings, θ_e was advected to higher levels for weak synoptic condition under both dry and wet soil moisture state. Overall, the dry cases largely resulted in reduced precipitation while in wet cases precipitation increased but not as spectacularly as expected. The latter occurred partly due to wet initial soil moisture conditions.

In summary, the model was able to capture the main precipitation signatures for three distinct precipitation events during the month of June 2006 and that the results of this study are robust within the synoptic conditions for this period. In our opinion, these findings are very relevant for better understanding of soil moisture and land-surface-atmosphere interactions. Moreover, these results can have impor- tant implications in applications of mesoscale models for practical purposes such as air quality studies which rely on accurate meteorological fields to compute trans- port and dispersion of pollutants.

REFERENCES

Aligo, E. A., Gallus, W. A., and Segal, M. (2007) Summer rainfall forecast spread in an ensemble initialized with different soil moisture analyses. *Weather and Forecasting*, Vol. 22, 299–314.

Alonge, C. J., Mohr, K. I., and Tao, W-K. (2007) Numerical studies of wet versus dry soil regimes in the West African Sahel. *Journal of Hydrometeorology*, Vol. 8, 102–116.

Anthes, R. A. (1984) Enhancement of convective precipitation by mesoscale variations in vegetative covering in semiarid regions. *Journal of Applied Meteorology*, Vol. 23, 541–554.

Avissar, R. and Liu, Y. (1996) Three-dimensional numerical study of shallow convective clouds and precipitation induced by land surface forcing. *Journal of Geophysical Research*, Vol. 101, 7499–7518.

Beljaars, A. C. M., Viterbo, P., Miller, M. J., and Betts, A. K. (1996) The anomalous rainfall over the United States during July 1993: Sensitivity to land surface parameterization and soil moisture anomalies. *Monthly Weather Review*, Vol. 124, 362–383.

Betts, A. K., Ball, J. H., Beljaars, A. C. M., Miller, M. J., and Viterbo, P. A. (1996) The land surface-atmosphere interaction: A review based on observational and global perspectives. *Journal of Geophysical Research*, Vol. 101, 7209–7225.

Brubaker, K. L., Entekhabi, D., and Eagleson, P. S. (1993) Estimation of continental precipitation recycling. *Journal of Climate*, Vol. 6, 1077–1089.

Chen, F. and Dudhia, J. (2001) Coupling an advanced land surface-hydrology model with the Penn State-NCAR MM5 modeling system Part I: model implementation and sensitivity. *Monthly Weather Review*, Vol. 129, 569–585.

Cheng, W. Y. Y. and Cotton, W. R. (2004) Sensitivity of cloud-resolving simulation of the genesis of a mesoscale convective system to horizontal heterogeneities in soil moisture initialization. *Journal of Hydrometeorology*, Vol. 5, 934–958.

Clark, C. A. and Arrit, R. W. (1995) Numerical simulations of the effect of soil moisture and vegetation cover on the development of deep convection. *Journal of Applied Meteorology*, Vol. 34, 2029–2045.

Delworth, T. L. and Manabe, S. (1988) The influence of soil wetness on near-surface atmospheric variability. *Journal of Climate*, Vol. 2, 523–547.

Ek, M. and Holstag, A. A. M. (2004) Influence of soil moisture on boundary layer development. *Journal of Hydrometeorology*, Vol. 5, 86–99.

Ek, M. and Mahrt, L. (1994) Daytime evolution of relative humidity at the boundary layer top. *Monthly Weather Review*, Vol. 122, 2709–2721.

Findell, K. L. and Eltahir, E. A. B. (1997) An analysis of the soil moisture-rainfall feedback, based on direct observations from Illinois. *Water Resources Research*, Vol. 33, 725–737.

Findell, K. L. and Eltahir, E. A. B. (2003) Atmospheric controls on soil moisture-boundary layer interactions: Three-dimensional wind effects. *Journal of Geophysical Research*, Vol. 108, No. D8,8385. DOI: 10.1029/2001JD001515.

Giorgi, F., Mearns, L. O., Shields, C., and Mayer, L. (1996) A regional model study of the importance of local versus remote controls of the 1988 drought and 1993 flood over the central United States. *Journal of Climate*, Vol. 9, 1150–1162.

Grunmann, P. J. (2005) Variational Data Assimilation of Soil Moisture Information. Unpublished doctorate thesis. Department of Meteorology, University of Maryland.

Hong, S-Y. and Pan, H-L. (1996) Nonlocal boundary layer vertical diffusion in a medium-range forecast model. *Monthly Weather Review*, Vol. 124, 2322–2339.

Jacobson, M. Z. (1999) Effects of soil moisture on temperatures, winds, and pollutant concentrations in Los Angeles. *Journal of Applied Meteorology*, Vol. 38, 607–616.

Kain, J. (2004) The Kain-Fritsch convective parameterization: An update. *Journal of Applied Meteorology*, Vol. 43, 170–181.

Kentucky Climate Center. (2008) Accessed in February 2008 from kyclim.wku.edu

Koster, R. D., Dirmeyer, P. A., Hahmann, A. N., Ijpelaar, R., Tyalha, L., Cox, P., and Suarez, M. J. (2002) Comparing the degree of land-atmosphere interaction in four atmospheric general circulation models. *Journal of Hydrometeorology*, Vol. 3, 363–375.

Lawrence, D. M. and Slingo, J. M. (2005) Weak land-atmosphere coupling strength in HadAM3: The role of soil moisture variability. *Journal of Hydrometeorology*, Vol. 6, 670–680.

Lanicci, J. M., Carlson, T. N., and Warner, T. T. (1987) Sensitivity of the Great Plains severe-storm environment to soil-moisture distribution. *Monthly Weather Review*, Vol. 115, 2660–2673.

Mahmood, R. and Hubbard, K. G. (2004) An analysis of simulated long-term soil moisture data for three land uses under contrasting hydroclimatic conditions in the northern Great Plains. *Journal of Hydrometeorology*, Vol. 5, 160–179.

Mesinger, F., DiMego, G., Kalnay, E., Mitchell, K., Shafran, P. C., Ebisuzaki, W., Jovi, D., Woollen, J., Rogers, E., Berbery, E. H., Ek, M. B., Fan, Y., Grumbine, R., Higgins, W., Li, H., Ying, L., Manikin, G., Parrish, D., and Shi, W. (2006) North American Regional Reanalysis. *Bulletin of the American Meteorological Society*, Vol. 87, 343–360.

Mintz, Y. (1984) The sensitivity of numerically simulated climates to land-surface boundary conditions. In J. Houghton, ed., *The Global Climate*. Cambridge, MA: Cambridge University Press, 79–105.

Ookuchi, Y., Segal, M., Kessler, R. C., and Pielke, R. A. (1984) Evaluation of soil moisture effects on the generation and modification od mesoscale circulations. *Monthly Weather Review*, Vol. 112, 2281–2292.

Pal, J. S. and Eltahir, E. A. B. (2001) Pathways relating soil moisture conditions to future summer rainfall within a model of the land-atmosphere system. *Journal of Climate*, Vol. 14, 1227–1242.

Pielke, R. A. (2001) Influence of the spatial distribution of vegetation and soils on the prediction of cumulus convective rain. *Reviews of Geophysics*, Vol. 39, 151–177.

Schar, C., Luthi, D., and Beyerle, U. (1999) The soil-precipitation feedback: A process study with a Regional Climate Model. *Journal of Climate*, Vol. 12, 722–741.

Schrieber, K., Stull, R., and Zhang, Q. (1996) Distributions of surface-layer buoy-
    ancy versus lifting condensation level over a heterogeneous land surface. *Journal
    of the Atmospheric Sciences*, Vol. 53, 1086–1107.
Segal, M. and Arrit, R. W. (1992) Non-classical mesoscale circulations caused by
    surface sensible heat-flux gradients. *Bulletin of the American Meteorology Soci-
    ety*, Vol. 73, 1593–1604.
Segal, M., Arrit, R. W., Clark, C., Rabin, R., and Brown, J. (1995) Scaling evaluation
    of the effect of surface characteristics on potential for deep convection over uni-
    form terrain. *Monthly Weather Review*, Vol. 123, 383–400.
Sutton, C., Hamill, T. M., and Warner, T. T. (2006) Will perturbing soil moisture
    improve warm-season ensemble forecasts? A proof of concept. *Monthly Weather
    Review*, Vol. 134, 3174–3188.
Ulack, R., Raitz, K., and Pauer, G. (1998) *Atlas of Kentucky*. Lexington, KY: The
    University Press of Kentucky.